Noise-Induced versus Intrinsic Oscillation in Ecological Systems

Shadisadat Esmaeili[1],
sesmaeili@ucdavis.edu
Alan Hastings[1,4],
amhastings@ucdavis.edu
Karen C. Abbott[2],
kca27@case.edu
Jonathan Machta[3,4],
machta@umass.edu
Vahini Reddy Nareddy[3],
vnareddy@umass.edu

[1] Department of Environmental Science and Policy, University of California, Davis, CA 95616, USA
[2] Department of Biology, Case Western Reserve University, Cleveland, OH 44106, USA
[3] Physics Department, University of Massachusetts, Amherst, MA 01003, USA
[4] Santa Fe Institute, Santa Fe, NM 87501

Short title:

Noise-Induced vs Intrinsic Oscillation

Authorship Statement

SE, designed the methodology, performed software development and simulations and data analysis, and wrote the original draft of the manuscript. AH, KA, and JM contributed to the conceptualization and methodology, and VRN contributed to the methodology. All authors contributed substantially to reviewing and editing of the manuscript.

Data Accessibility Statement: No new data were used.

Keywords:

Noise-induced, Oscillation, Synchrony, Spatiotemporal, phase transition

Type of Article: Letters

# of words:
Abstract: 149
Main Text: 4495
# of figures: 6 (No tables or text boxes)
# of references: 63

Corresponding Author:

Shadi Esmaeili
(540)818-3088
sesmaeili@ucdavis.edu
mailing address: 413 River Birch Ln., Fleming Island, Fl 32003

Abstract

Studies of populations oscillating through time have a long history in ecology as these dynamics can help provide insights into the causes of population regulation. A particularly difficult challenge is determining the relative role of deterministic versus stochastic forces in producing this oscillatory behavior. Another classic ecological study area is the study of spatial synchrony which also has helped unravel underlying population dynamic principles. One possible approach to understanding the causes of population cycles is based on the idea that a focus on spatiotemporal behavior, oscillations in coupled populations, can provide much further insight into the relative role of deterministic versus stochastic forces. Using ideas based on concepts from statistical physics, we develop results showing that in a system with coupling between adjacent populations, a study of spatial synchrony provides much information about the underlying causes of oscillations. Novel, to ecology, measures of spatial synchrony are a key step.

1 Introduction

Cyclic or oscillatory dynamics are prevalent in nature and are observed in a variety of fields. Well-known examples are fluctuations of different species' population numbers (Benincà et al., 2015; Turchin and Ellner, 2000; Elton, 1924), predator-prey dynamics (Gurney and Nisbet, 1978), insect outbreaks (Blackwood et al., 2018), oscillatory behavior in plant seed production (Noble et al., 2018; Lyles et al., 2015; Shalom et al., 2012), the circadian pacemaker cells (Gonze et al., 2018), oscillating chemical reactions (Simokov and Pérez-Mercader, 2013), neural systems (Tchumatchenko and Clopath, 2014; Galán et al., 2006), and epidemiological systems (Chaffee and Kuske, 2011; Rohani et al., 1999).

Among ecologists, the mechanisms behind these fluctuations are of great interest and have been the topic of many studies drawing on short-term experiments and observations, statistical analysis of long time series, and mathematical modeling (Berryman, 2002; Krebs et al., 2001; Kendall et al., 1999; Nisbet and Gurney, 1976; Elton, 1924). Four major mechanisms have been identified for these fluctuations: environmental stochasticity (Lugo and McKane, 2008; Nisbet and Gurney, 1982, 1976), periodic extrinsic conditions (e.g. weather patterns and seasonality) (Hunter and Price, 1998; Sinclair et al., 1993; Elton, 1924), intrinsic ecological interactions and internal dynamics, like density dependence and consumer-resource interactions (Esmaeili et al., 2021; Kendall et al., 1999; Isagi et al., 1997; May, 1972), and physiological and demographic evolution (Barraquand et al., 2017). Given the stochastic nature of the ecological systems, discerning between different mechanisms producing oscillatory behavior has been challenging. In some cases, the oscillatory dynamics resulting from different processes appear to be similar. External noise can make qualitative changes to the limit cycles and create fluctuations in an otherwise stable focus by repeated random excitation (Barraquand et al., 2017). A deterministic limit cycle (or a two-cycle behavior) is called an intrinsic oscillator, but when the deterministic skeleton is a stable focus, the observed fluctuations are noise-induced. Under the effect of a strong noise, an intrinsic oscillator (i.e. deterministic limit cycle) can have similar distribution to a noise-induced oscillator (i.e. stable focus) (Lin and Kahn, 1977; Nisbet and Gurney, 1976). Since the majority of ecological dynamics data are time series, different ways have been proposed to distinguish between oscillatory behaviors prompted by different mechanisms, all using time series analysis of a single oscillator. These methods include using the response of the system to a random perturbation (Louca and Doebeli, 2014), combined analysis of autocorrelation and marginal distributions in a predator-prey system (Pineda-Krch et al., 2007), and replacing the white noise with a generalized noise with temporal correlation as a point of reference to compare against the oscillatory behavior observed in the time series (Louca and Doebeli, 2015). However, as Hunter and Price (1998) suggested, using time series analysis can be insufficient to gain information regarding the cause of the oscillatory behavior and can lead to spurious results.

Beyond time series analysis, one of the intriguing features of oscillatory ecological systems is the ubiquitous spatial synchronization and the formation of spatial patterns which can provide more information about underlying mechanisms. Population sizes, reproductive behavior (mast seeding in plants), mortality, and other characteristics of populations are observed to be spatially correlated (Liebhold et al., 2004). Dispersal

(Wall et al., 2013; Goldwyn and Hastings, 2008; Stone et al., 2002; Blasius and Stone, 2000), direct or indirect trophic interactions (Selås, 1997; Satake et al., 2004), shared moving predator (Ims and Andreassen, 2000; Small and Willebrand, 1993), and synchronous stochastic external (weather) effects (Koenig, 2002; Moran, 1953) can each cause synchronization and formation of long-range correlation. While each of these mechanisms is considered as a candidate to promote synchrony, in some cases the nontrivial interaction between two or more of these factors is necessary to explain observed synchrony (Kendall et al., 2000). Traditionally, assessing synchrony has been done by measuring the correlation coefficients between pairs of population time series (Liebhold et al., 2004; Greenman and Benton, 2001), the residual from a fitted model (Buonaccorsi et al., 2001), or the covariance function between population time series (Bjørnstad and Falck, 2001). In some studies the coincidence of peaks or the proportion of times when the time series go up and down together is used as the measure of synchrony (Buonaccorsi et al., 2001). All these measurements are pairwise. When the system includes more than two time series, the measures are averaged over all the existing pairs in the system. However, inspired by statistical physics models, Noble et al. (2015), took a different approach and used the concept of the order parameter (Newman and Barkema, 2001; Goldenfeld, 1992) to measure the global degree of synchrony for discrete-time two-state systems.

In this paper, we approach the question of distinguishing between noise-induced and intrinsic oscillators through the lens of collective dynamics and synchronization and ask whether the collective dynamics offer indirect information into the mechanism behind ecological cycles. We use an ecological model that shows period-doubling bifurcations and models the fluctuating yield in alternate bearing plants (Esmaeili et al., 2021). Alternate-year masting is one example of an ecological two-cycle that has been used previously to understand the interplay between stochasticity and nonlinearity and their effect on synchronization in population dynamics (Lyles et al., 2015, 2009). We compare the behavior of the model in the stable fixed point regime (noise-induced oscillations) with its dynamics in the two-cycle regime (intrinsic oscillations) at different spatial scales of observation (figure 1). We start by analysing the time series for a single oscillator in an isolated setting (figure 1a) or inside a population or metapopulation (lattice) where the individuals interact with each other via root-grafting or pollen coupling (figure 1b). We expand our scale by looking at a two-oscillator system (figure 1c, d, & e) as well as the collective behavior of the entire lattice (figure 1f). When the scale of observation is larger than one oscillator, we use two measures of synchrony, Degree of Agreement (Buonaccorsi et al., 2001) and Synchronization Order Parameter (Noble et al., 2015), to compare the dynamics of noise-induced and intrinsic oscillators. The Degree of Agreement is a pairwise measurement, which measures the global synchrony by averaging over all the pairs, while the Synchronization Order Parameter measures the global synchrony directly. Lattice models with a two-cycle, and the ecological systems represented by them, have been shown to go through a transition from synchrony to disorder as the level of stochasticity changes (Noble et al., 2015), a second order phase transition (Solé, 2011; Goldenfeld, 1992). For given values of the model's parameters there is a critical noise intensity below which the system's asymptotic state is synchrony and beyond which the system is spatially disordered. On a parameter phase

diagram, the critical noise value as a function of the model's parameter forms a boundary between the ordered and disordered phases (i.e. a critical line). Our results show that noise intensity plays an important role and can become the dominant driver of the oscillations even if the deterministic skeleton is in the two-cycle regime. Our results suggest that the critical line separating the two phases on the parameter phase diagram (which includes the effect of stochasticity) is a better guide to determine the driving force of the oscillations than the deterministic bifurcation point.

2 Model and Simulation

We use stochastic, discrete-time ecological models to investigate the characteristics of noise-induced versus noisy intrinsic oscillators. We study the individual oscillators as well as the collective behavior on a coupled map lattice. A coupled map lattice under the effect of noise can be written as,

$$s_{i,t+1} = (1-\kappa) f(s_{i,t}, \boldsymbol{\xi}_{i,t}) + \frac{\kappa}{N_i} \sum_j f(s_{j,t}, \boldsymbol{\xi}_{j,t}), \tag{1}$$

where $s_{i,t}$ is the state at the location i at time t, κ is a measure of the coupling strength between the adjacent sites on a lattice with $L_x \times L_y$ oscillators, and N_i is the number of nearest neighbors ($N_i = 4$ on a square lattice).

The function $f(s_t)$ is a deterministic overcompensatory density-dependent map that models the internal dynamics at each location. Maps such as Ricker (Ricker, 1954) and logistic, as well as the Density Dependent Resource Budget Model (DDRBM) (Esmaeili et al., 2021), describe many ecological systems. Their bifurcation diagrams show a period-doubling route to chaos as the function of the models' growth parameter (r). The term $\boldsymbol{\xi}_t$ represents Gaussian noise with mean zero and variance σ^2 to model environmental stochasticity. In this paper, the standard deviation, σ, is referred to as the noise intensity.

We consider an oscillation to be noise-induced if the fluctuations are only noise driven. This happens when the parameter of the deterministic map is in the fixed point regime and the system approaches the fixed point with damped oscillations. However, noisy intrinsic oscillators are ones for which the deterministic skeleton shows an oscillatory behavior and the presence of the noise impacts the phase and amplitude of the already existing oscillation. In this case, the parameter is in the two-cycle regime.

The results presented in this paper are ensemble averages obtained from 100 realizations of the DDRBM described in Esmaeili et al. (2021) and Appendix A. However, the general approach can be applied to other overcompensatory density-dependent ecological maps, as we illustrate with the Ricker map (Appendix B). We compare the dynamics in the stable regime with those in the two-cycle regime for different spatial scales of observation (a single tree, a two-tree system, and an orchard). The orchard simulations are done on a $N = 32 \times 32$ lattice with nearest neighbor coupling ($\kappa = 0.15$) and free boundary conditions (trees located at the edges share their resources with only three neighbors). Further simulation details can be found in Appendix A.

2.1 Synchronization and Phase Transition

At the collective level, ecological models, in their two-cycle regime go through a critical phase transition from synchrony to disorder as the noise intensity increases (Noble et al., 2015). The critical noise value where the transition happens is a function of the model's parameter and the coupling strength. The $r - \sigma$ phase diagram of the DDRBM for $\kappa = 0.15$ is shown in figure 1f. The line that separates the two phases is the critical line. When the parameters are in the vicinity of the critical line, large fluctuations which are correlated over the long distances are observed in the system. The phase transition phenomenon is observed in a variety of systems in different fields (e.g. magnetic systems, liquid gas, etc.) (Goldenfeld, 1992; Cardy, 1996; Solé, 2011). To detect the phase transition, we need to measure the degree of synchrony in the system. In this paper we use two measures of synchrony: the Synchronization Order Parameter (a global measurement) (Noble et al., 2015) and the Degree of Agreement (a pairwise measurement) (Buonaccorsi et al., 2001).

Synchronization Order Parameter

We use the synchronization order parameter as defined in Noble et al. (2015) and inspired by its use in statistical physics. A magnetic system, modeled with Ising model (Goldenfeld, 1992), is composed of N magnetic dipole moments (spins) that can be in either an "up" $(+1)$ or "down" (-1) state. The order parameter or magnetization of such systems is defined by the average over all the spins. A magnetization of either $+1$ or -1 indicates perfect order in the system where all the spins are aligned and the magnetization near zero shows complete disorder.

In the context of two-cycle ecological oscillators, each oscillator is assigned a two-cycle variable,

$$m_{i,t} = (-1)^{t+1}(s_{i,t+1} - s_{i,t})/2. \tag{2}$$

Here $m_{i,t}$ has information about the amplitude and the phase of the oscillator. The phase of the oscillator refers to whether the maximum happens in odd or even time steps (arbitrarily called positive or negative phase, respectively) and is equivalent to the $+1$ or -1 spin in a magnetic system. Oscillators i and j are in synchrony if $m_{i,t}m_{j,t} > 0$. The spatial average of equation 2, over the entire lattice, gives us the Instantaneous Order Parameter,

$$\text{Instantaneous Order Parameter} = \frac{1}{N}\sum_{i=1}^{N} m_{i,t}, \tag{3}$$

where $N = L_x \times L_y$ is the total number of the oscillators on the lattice. To measure the Synchronization Order Parameter, we take a time average of the absolute value of equation 3,

$$\text{Synchronization Order Parameter} = \frac{1}{T - T_b - 1}\sum_{t=T_b}^{T-1}\left|\frac{1}{N}\sum_{i=1}^{N} m_{i,t}\right|, \tag{4}$$

where T_b is the waiting time to allow the system to reach the stationary state and T is the total observation time.

Degree of Agreement

Buonaccorsi et al. (2001) defined the Degree of Agreement for two fluctuating time series to measure the average number of time steps where the two oscillators change in the same direction, which reflects the degree of synchrony between them. Two time series change in the same direction from time t to time $t+1$ if the product of their first difference is positive ($d_{i,t}d_{j,t} > 0$, where $d_{i,t} = s_{i,t+1} - s_{i,t}$). We define,

$$A_{ij,t} = \begin{cases} 1, & d_{i,t}d_{j,t} > 0 \\ 0 & \text{otherwise.} \end{cases} \tag{5}$$

Therefore, in the context of this study, the Degree of Agreement for two oscillators can be written as

$$A_{ij} = \frac{1}{T - T_b - 1} \sum_{t=T_b}^{t=T-1} A_{ij,t}. \tag{6}$$

The Degree of Agreement for a lattice is the pairwise average,

$$\text{Degree of Agreement} = \frac{1}{N(N-1)/2} \sum_i \sum_{j<i} A_{ij}, \tag{7}$$

which is expected to have a minimum around 0.5, since independent oscillators will be in-phase by chance 50% of the time.

3 Results

3.1 Individual Oscillator

Isolated Oscillator

We start with the simplest case of an isolated tree, as it provides information regarding the internal dynamics in different regimes under the effect of noise. The time series obtained from an individual oscillator in the fixed point (noise-induced oscillations, $r < 6.8$) and two-cycle (noisy intrinsic oscillations, $r > 6.8$) regimes increasingly resemble each other as stochasticity increases (figure 2, top panel in each box).

When environmental stochasticity is small, the deterministic skeleton of the tree's internal dynamics can be detected by looking at its power spectrum (third panels, figure 2a-f) and autocorrelation function (fourth panels). However, for the larger noise intensities, the transient two-cycles in the stable regime are continually re-excited, and intrinsic two-cycles in the cyclic regime are masked by the environmental fluctuations. Therefore, the distinction between the noise-induced and noisy intrinsic oscillation becomes more obscure and difficult to detect (figure 2c & f).

The autocorrelation (AC) of the resource level of the tree in the two-cycle regime ($r = 7.1$), with weak noise, shows a steady oscillation. However, as the environmental noise becomes stronger, noise becomes the dominant driver in the dynamics of the tree's resource levels, resulting in damped oscillations with a characteristic time that decreases with increasing noise intensity (figure 2d-f, fourth panels). For a tree in

the fixed point regime ($r = 6.5$), environmental noise is the cause of the observed oscillations and therefore, its autocorrelation decays with the characteristic time inversely related to the noise intensity (figure 2). The relationship between the characteristic time and the noise intensity of noise-induced and noisy intrinsic oscillators are shown in Appendix E.

Lastly, a change in the sign of the two-cycle variable, $m_{i,t}$, represents the change in the phase of the oscillation (color coded in figure 2, top two panels). The distribution of the two-cycle variable clearly distinguishes noise-induced and intrinsic oscillations. For the noise-induced oscillator, $m_{i,t}$ shows an approximately Gaussian distribution centered on zero whose width increases with noise intensity. For the noisy intrinsic oscillator, there are two distinct phases of oscillations and the noise causes the oscillator to switch between the two phases, therefore, the distribution is bi-modal. When the noise is weak, the bi-modality is hidden because the switching time between the phases exceeds the observation time but is nonetheless implied by the displacement of the single peak from the origin together with the required symmetry of the distribution. As noise becomes more dominant, large fluctuations are reflected in the form of a bi-modal distribution with two connected peaks (figure 2e). Under the effect of strong noise, the distribution approaches Gaussian with fat tales. A more detailed study of the evolution of this distribution under the effect of noise can be found in Noble et al. (1990).

Individual Oscillator on a Lattice

To make our analysis more relevant to real-world systems, we now study an individual tree that is part of an orchard (figure 1b). The chosen tree is far from the boundary of the lattice and is coupled to its four nearest neighbors. For parameter values (r and σ) that fall above the critical line (figure 3 center plot, solid line), the entire orchard is synchronized and all the trees are collectively in either the positive or negative phase of oscillation; otherwise, the orchard is spatially disordered. Notice that this critical line is distinct from the deterministic bifurcation point (dashed line) that determines whether oscillations are noise-induced or intrinsic, though the two lines are expected to meet at zero noise.

At the first glance, the power spectrum and autocorrelation of a tree in a lattice (figure 3) appear similar to that of an isolated tree. The internal dynamics of the oscillator under the weak stochastic effects is evident from its power spectrum and autocorrelation function (figure 3 left two panels). As the noise increases and becomes dominant, the internal dynamics are masked and undetectable (figure 3 right two panels). In the transition from weak to strong noise, the power spectrum becomes noisier and the characteristic autocorrelation time decreases. The deterministic bifurcation line divides noise-induced from intrinsic cycles, but when noise dominates the dynamics, the difference may not be detectable. In contrast, the critical line divides these noise dominant dynamics from dynamics ordered by internal processes. As such, it is the critical line rather than the bifurcation point that corresponds to a significant change. While in the case of the isolated oscillator, any amount of noise will eventually change the phase of the oscillator and therefore lead to the decay of the autocorrelation function, but an oscillator inside the lattice in the synchronized regime is protected from noise and any occasional switching of the phase due to noise is restored by the collective

dynamics of the entire lattice. As we increase the noise while r is still in the two-cycle regime, the entire orchard goes through a phase transition and the competition between the coupling, internal dynamics, and the environmental noise becomes more fierce. As we increase the noise further into the disordered regime, while the environmental noise is not the driver of the oscillations (as it is in the fixed point regime), it is dominating the internal dynamics. Therefore the characteristics of the oscillations (power spectrum and autocorrelation) resembles the ones where r is below the bifurcation point. The power spectrum shows concentrated fluctuations close to the two-cycle frequency and the autocorrelation shows decaying oscillations.

The distribution of the two-cycle variable, $m_{i,t}$, in the fixed point regime (green dots in figure 4a) is Gaussian with kurtosis equals zero and the width of the distribution increasing with the noise intensity. (See Appendix C for a detailed explanation of the relationship between the kurtosis and the Binder Cumulant, another well-known quantity from statistical physics.) On the other hand, following the path of the blue stars, the kurtosis starts from zero when $r = 6.5$ and becomes more and more negative as we increase r and move toward the critical line reaching its lowest value when the parameter falls on the critical line (figure 4c). As r increases and crosses the deterministic bifurcation line the distribution changes from normal to a wide distribution with narrow tails (platykurtic) and finally becoming bi-modal as we approach the critical line. As we cross the critical line into the synchronized phase, the kurtosis suddenly becomes positive and the distribution shows a skewed long-tailed distribution with an off-zero mean. In the ordered phase, where all the oscillators are synchronized, an individual oscillator maintains its phase and the change of sign of the two-cycle variable happens with a very small probability.

Analyzing an individual oscillator as part of the collective and in the context of the phase transition offers some new insights into the categorization of "Noise-Induced" and "Noisy Intrinsic" oscillator. What we see from both figures 3 and 4 is that the behavior of the system is very similar as long as the parameters are in the disordered phase. While continuous changes can be detected as we cross the deterministic bifurcation line, the sharp, hard-to-miss transition happens when the parameter cross the critical line and the system transitions into the ordered regime.

3.2 Two-Oscillator System

In the previous sections, we used time series analysis to study the oscillatory behavior of an individual tree. However, the spatiotemporal patterns (like synchrony) that are observed in the collective dynamics of the communities can provide indirect information about the main driver of the observed fluctuations. In this section, we start with the smallest size of community, a system consisting of two coupled trees (figure 1c). Then, we consider the behavior of two nearest neighbor (figure 1d) and non-nearest neighbor trees (figure 1e) in an orchard.

Isolated Coupled Pair of Oscillators

Figure 5a and b show the Synchronization Order Parameter (figure 5a) and the Degree of Agreement (figure 5b) as functions of r (the growth rate) and σ (the noise intensity). The green shaded area in both figures

shows the fixed point regime where the noise-induced oscillation happens. The blue shaded area illustrates the two-cycle regime where the intrinsic oscillations exist. We can see a noticeable change in the degree of synchronization, observed in both measures of synchrony, around the deterministic bifurcation point when the noise is weak. Synchrony is only achieved when the internal dynamics of oscillators are in the two-cycle regime and not masked by strong stochastic effects. Purely noise-induced oscillators with this degree of coupling do not synchronize regardless of the level of stochasticity. However, this distinction is obscured as stochasticity weakens synchrony in the two-cycle regime.

The increase of the Synchronization Order Parameter with the noise intensity (σ), when $r < 6.8$, is an artifact related to the definition of the Synchronization Order Parameter and the two-cycle variable and is not an indication of increased synchronization. As the noise gets stronger, it causes oscillations with larger amplitudes and therefore larger $m_{i,t}$ associated with each tree. This results in larger values of the Synchronization Order Parameter. This effect is not present in figure 5b, since the Degree of Agreement is independent of the amplitude of the oscillations.

Two-Oscillator Dynamics on a Lattice

In an orchard, the dynamics of neighboring trees (figures 5c and 5d) are close to the dynamics of the isolated pair discussed in the previous section. For non-neighboring trees, there is a sharper transition from in-phase to out-of-phase for all values of the noise (figures 5e and 5f). As the noise increases the transition happens at a larger r inside the two-cycle regime. The transition from synchrony to disorder observed in the measure of synchrony of the two non-neighboring trees matches the critical line on the parameter phase diagram. The smoother and more gradual transition from synchronization to disorder in the neighboring trees, under strong noise, is due to the direct coupling between the two trees. The two neighboring trees become correlated before the long-range correlation is formed in the entire lattice (as we will discuss in the next section). Also, because the Degree of Agreement, by definition, is independent of the amplitude of the oscillations, the transition from the in-phase state to out-of-phase state appear to be sharper compared to the Synchronization Order Parameter.

3.3 Collective Dynamics of Coupled Oscillators on a Lattice

The phase transition from synchrony to disorder in the two cycle regime is most clearly observed when the entire lattice is taken into account (figure 6), which show the behavior of the Synchronization Order Parameter and the Degree of Agreement in the entire lattice. In the ordered (synchronized) regime, the internal dynamic of the trees (two-cycle behavior) and the nearest-neighbor coupling overcome the effect of the stochasticity. As a result, long-range correlation is formed across the lattice and the orchard becomes synchronized. This feature gives us information about the deterministic skeleton of the system. If an entire system is synchronized, the individual units are intrinsic oscillators. However, the converse is not necessarily true. In the disordered phase, noise becomes the dominant driver of the dynamics and overcomes the coupling and any internal two-cycle behavior of each unit and the synchronization cannot be achieved. Both measures

of synchrony rise sharply at the transition from disordered to synchrony. These results tell us that, at the collective level, the measures of synchrony cannot distinguish between the noise-induced and noise dominated dynamics.

4 Discussion

In this paper, we reframed the problem of distinguishing between noise-induced and intrinsic oscillators and asked whether noise is the driver of the observed dynamics. This question can be discussed in terms of the competition between the internal dynamics and the coupling (in the case of spatially extended systems) on one hand and stochasticity on the other hand. At all scales of observation, once the external noise becomes the dominant driver of the dynamics, distinguishing between different deterministic skeletons becomes challenging. At the collective level, synchronization and the formation of spatial patterns can provide indirect information about the driver of the observed fluctuations. Spatially extended intrinsic oscillators (unlike noise-induced oscillators), can readily synchronize due to local coupling under the effect of weak noise. As the level of stochasticity increases, the system goes through a phase transition. Beyond the critical value of the noise, the synchronization collapses into complete disorder. However, if the noise is the source of the fluctuations, the system cannot synchronize and remains in the state of disorder independent of the noise intensity (i.e., there is no phase transition).

Ecologists use oscillatory behavior observed in ecological systems to learn about the forces behind these oscillations (Hunter and Price, 1998; Elton, 1924). Many studies have analyzed the time series obtained from the real systems (or ecological models) to match the stochastic behavior to their deterministic mechanisms. However, due to inherent stochasticity of the ecological systems, many of the identified mechanisms behind the oscillatory behavior result in very similar dynamics and therefore, the time series analysis approach can be insufficient. We used a spatially extended discrete time noisy ecological model with a period-doubling bifurcation and compared the dynamics of the system in the stable fixed point regime versus its dynamics in the two-cycle regime. At the level of an individual oscillator, the distribution of the two-cycle variable can provide the most insights into the mechanisms behind the observed fluctuations. While the distribution is Gaussian if the noise is the only cause of fluctuations, in the two-cycle regime the distribution becomes bimodal as long as the noise has not overcome the internal two-cycle dynamics. At the collective level, we used two measurements of synchrony: the Degree of Agreement which is a pairwise measurement of synchrony, and the Synchronization Order Parameter which measures the global degree of synchronization across the lattice. We showed that if the system consists of coupled intrinsic oscillators synchronization can be achieved if the noise is not overpowering the internal dynamics. This feature is not observed in a system made of coupled noise-driven oscillators.

Applying what we learn from ecological models to real systems is always accompanied with limitations and compromises. To analyze the spatiotemporal characteristics of the system, the Synchronization Order Parameter and the Degree of Agreement are measured asymptotically. The time that it takes for the system

to reach the asymptotic state (equilibrium) is a function of the system's size and the initial conditions. The closer the system is to its equilibrium state the shorter the time to reach equilibrium. In this paper, our choice of the initial conditions in the vicinity of the disordered regime has inevitably lengthened the relaxation time to reach the ordered steady state. In many ecological systems, an initial state closer to the ordered state might be considered more realistic since a sudden perturbation can have synchronizing effect and reset the clock of the individual oscillators. However, since all our measurements are done in equilibrium, the final results are independent of the initial conditions and our results can be applied to different initial conditions (Appendix C). Depending on the specific ecological system under investigation, the system size used in this paper can be considered too large, or too small. The relationship between the system size and the time to reach equilibrium is well-studied in the statistical physics (Lin and Wang, 2016; Walter and Barkema, 2015; Oerding, 1995) . At the critical regime the time that it takes for the system to reach equilibrium increases as a power of the system size (Lin and Wang, 2016; Family, 1990). Smaller systems require shorter times to reach equilibrium, however, the smaller the system, the larger the statistical error will be. While working with models, averaging over many realization is used to minimize the statistical error, however, while working in real systems, this is not a practical approach. We showed in Appendix D that even without ensemble averaging, the results remain qualitatively unchanged.

The models studied in this paper are part of larger categories of systems. They are unimodal maps with period-doubling route to chaos. They go through a phase transition from synchrony to disorder. In their critical regime, the scaling behavior of their statistical quantities is similar to the Ising model of magnetic moments. Therefore, they belong to the Ising universality class (Noble et al., 2015; Solé, 2011; Cardy, 1996; Goldenfeld, 1992). These features allow us to generalize our results beyond the two models studied in this paper and expand our discussion to all the systems that can be described by models with a period doubling bifurcation (e.g logistic map, host-parasitoid model, etc). Synchronization and phase transition are observed in systems with different geometrical structures (Morita and Suzuki, 2016). While we performed our simulations on a square lattice, we believe the results are independent of the geometry of the system and can be applied to any oscillatory system that goes through a phase transition. The question of the mechanisms behind oscillatory behaviors observed in nature is an active question in a variety of fields. We believe our results can provide insight into this question for oscillatory systems where a transition from synchrony to disorder is observed.

Acknowledgement

This work is supported by NSF grant DMS-1840221.

References

F. Barraquand, S. Louca, K.C. Abbott, C.A. Cobbold, F. Cordoleani, D.L. DeAngelis, B.D. Elderd, J.W. Fox, P. Greenwood, F.M. Hilker, D.L. Murray, C.R. Stieha, R.A. Taylor, K. Vitense, G.S. Wolkowicz, and R.C. Tyson. Moving forward in circles: challenges and opportunities in modelling population cycles. *Ecol. Lett.*, 20:1074–1092, 2017.

E. Benincà, B. Ballantine, S. P. Ellner, and J. Huisman. Species fluctuations sustained by a cyclic succession at the edge of chaos. *PNAS*, 112(20):6389–6394, 2015.

A. A. Berryman. *Population cycles: cause and analysis. In: Population cycles: the case for trophic interactions.* Oxford Univ. Press, Oxford, 2002.

K. Binder. Finite size scaling analysis of ising model block distribution functions. *Z. Phys. B*, 43:119, 1981.

K. Binder and D.P. Landau. Finite-size scaling at first-order phase transitions. *Phys. Rev. B*, 30:1477, 1984.

O. Bjørnstad and W. Falck. Nonparametric spatial covariance functions: Estimation and testing. *Environ. Ecol. Stat.*, 8:53–70, 2001.

J. C. Blackwood, J. Machta, A. D. Meyer, A. E. Noble, A. Hastings, and A. M. Liebhold. Competition and stragglers as mediators of developmental synchrony in periodical cicadas. *Am. Nat.*, 192(4), 2018.

B. Blasius and L. Stone. Chaos and phase synchronization in ecological systems. *Int. J. Bifurc. Chaos*, 10 (10):2361–2380, 2000.

J. P. Buonaccorsi, J. S. Elkinton, S. R. Evans, and A. M. Liebhold. Measuring and testing for spatial synchrony. *Ecology*, 82(6):1668–1679, 2001.

J. Cardy. *Scaling and Renormalization in Statistical Physics.* Cambridge Univ. Press, Cambridge, 1996.

J. Chaffee and R. Kuske. The effect of loss of immunity on noise-induced sustained oscillations in epidemics. *Bull. Math. Biol.*, 73:2552–2574, 2011.

M. S. S. Challa, D. P. Landau, and K. Binder. Finite-size effects at temperature-driven first-order transitions. *Phys. Rev. B*, 34:1841, 1986.

C. Elton. Periodic fluctuations in the numbers of animals: their cause and effects. *Brit. J. Exp. Biol.*, 2: 119–163, 1924.

S. Esmaeili, A. Hastings, K. Abbott, J. Machta, and V. Reddy Narredy. Density dependent resource budget model for alternate bearing behavior. *Journal of Theoretical Biology*, 509:110498, 2021.

F. Family. Dynamic scaling and phase transitions in interface growth. *Physica A,*, 168:561–580, 1990.

R. F. Galán, N. Fourcaud-Trocmé, G. B. Ermentrout, and N. N. Urban. Correlation-induced synchronization of oscillations in olfactory bulb neurons. *J. Neurosci.*, 26(14):3646–3655, 2006.

N. Goldenfeld. *Lectures on Phase Transitions and the Renormalization Group*. Westview Press, Boulder, CO, 1992.

E. E. Goldwyn and A. Hastings. When can dispersal synchronize populations? *Theoretical Population Biology*, 73(3):395–402, 2008.

Di. Gonze, C. Gérard, B. Wacquier, A. Woller, A. Tosenberger, A. Goldbeter, and G. Dupont. Modeling-based investigation of the effect of noise in cellular systems. *Frontiers in Molecular Biosciences*, 5:34, 2018.

J. V. Greenman and T. G. Benton. The impact of stochasticity on the behaviour of nonlinear population models: synchrony and the moran effect. *Oikos*, 93:343–351, 2001.

W. S. C. Gurney and R. M. Nisbet. Predator-prey fluctuations in patchy environments. *J. Anim. Ecol.*, 47: 85–102, 1978.

M. D. Hunter and P. W. Price. Cycles in insect populations: delayed density dependence or exogenous driving variables? *Ecol. Ent.*, 23(2):216–222, 1998.

R. A. Ims and H. P. Andreassen. Spatial synchronization of vole population dynamics by predatory birds. *Nature*, 408:194–196, 2000.

Y. Isagi, K. Sugimura, A. Sumida, and H. Ito. How does masting happen and synchronize? *J. Theor. Biol.*, 187:231–239, 1997.

B. E. Kendall, C. J. Briggs, W. W. Murdoch, P. Turchin, S. P. Ellner, E. McCauley, R. M. Nisbet, and S. N. Wood. Why do populations cycle? a synthesis of statistical and mechanistic modeling approaches. *Ecology*, 80(6):1789–1805, 1999.

B. E. Kendall, O. N. Bjjørnstad, J. Bascompte, T. H. Keitt, and W. F. Fagan. Dispersal, environmental correlation, and spatial synchrony in population dynamics. *Am. Nat.*, 155(5):628–636, 2000.

W. D. Koenig. Global patterns of environmental synchrony and the moran effect. *Ecography*, 25:283–288, 2002.

C. J. Krebs, R. Boonstra, S. Boutin, and A.R.E. Sinclair. What drives the 10-year cycle of snowshoe hares? *BioSci.*, 15(1):25–35, 2001.

M. Ladrem, M. A. A. Ahmed1, Alfull1 Z. Z., and S. Cherif. Finite-volume cumulant expansion in qcd-colorless plasma. *Eur. Phys. J. C*, 75:431, 2015.

A. Liebhold, W. D. Koenig, and O. N. Bjørnstad. Spatial synchrony in population dynamics. *Annu. Rev. Ecol. Evol. Syst.*, 35(1):467–490, 2004.

J. Lin and P. B. Kahn. Limit cycles in random environments. *SIAP*, 32(1):260–291, 1977.

Y. Lin and F. Wang. Linear relaxation in large two-dimensional ising models. *Phys. Rev. E*, 93:022113, 2016.

S. Louca and M. Doebeli. Distinguishing intrinsic limit cycles from forced oscillations in ecological time series. *Theor Ecol.*, 7:381–390, 2014.

S. Louca and M. Doebeli. Detecting cyclicity in ecological time series. *Ecology*, 96(6):1724–1732, 2015.

C. A. Lugo and A. J. McKane. Quasicycles in a spatial predator-prey model. *Phys. Rev. E*, 78:051911, 2008.

D. Lyles, T. S. Rosenstock, A. Hastings, and P. H. Brown. The role of large environmental noise in masting: General model and example from pistachio trees. *J. Theor. Biol.*, 259(4):701–713, 2009.

D. Lyles, T. S. Rosenstock, and A. Hastings. Plant reproduction and environmental noise: How do plants do it? *J. Theor. Biol.*, 371:137–144, 2015.

Robert M. May. Limit cycles in predator-prey communities. *Science*, 177(4052):900–902, 1972.

P. A. P. Moran. The statistical analysis of the canadian lynx cycle. ii. synchronization and meteorology. *Aust. J. Zool.*, 1:291–298, 1953.

S. Morita and S. Suzuki. Phase transition of two-dimensional ising models on the honeycomb and related lattices with striped random impurities. *J. Stat. Phys.*, 162:123–138, 2016.

V. R. Nareddy, J. Machta, K. C. Abbott, S. Esmaeili, and A. Hastings. Dynamical ising model of spatially coupled ecological oscillators. *J R Soc Interface*, 17:20200571, 2020.

M. E. J. Newman and G. T. Barkema. *Monte Carlo Methods in Statistical Physics*. Clarendon Press, Oxford, 2001.

R. M. Nisbet and W. S. C. Gurney. A simple mechanism for population cycles. *Nature*, 263:319, 1976.

R. M. Nisbet and W. S. C. Gurney. *Modelling fluctuating populations*. Wiley, 1982.

A. E. Noble, J. Machta, and A. Hastings. Emergent long-range synchronization of oscillating ecological populations without external forcing described by ising universality. *Nature Communications*, 6:6664, 2015.

A. E. Noble, T. S. Rosenstock, P. H. Brown, J. Machta, and A. Hastings. Spatial patterns of tree yield explained by endogenous forces through a correspondence between the ising model and ecology. *PNAS*, 115 (8):1825–1830, 2018.

A.E. Noble, S. Karimeddiny, A. Hastings, and J. Machta. Critical fluctuations of noisy period-doubling maps. *Eur. Phys. J. B*, 90, 1990.

K. Oerding. Relaxation times in a finite ising system with random impurities. *J. Stat. Phys.*, 78:893–916, 1995.

M. Pineda-Krch, H. J. Blok, Dieckmann U., and M. Doebeli. A tale of two cycles: Distinguishing quasi-cycles and limit cycles in finite predator-prey populations. *Oikos*, 116(1):53–64, 2007.

W. E. Ricker. Stock and recruitment. *Journal of the Fisheries Board of Canada*, 11(5):559–623, 1954.

P. Rohani, D. J. D. Earn, and B. T. Grenfell. Opposite patterns of synchrony in sympatric disease metapopulations. *Science*, 286(5441):968–971, 1999.

A. Satake, O. Bjørnstad, and S. Kobro. Masting and trophic cascades: interplay between rowan trees, apple fruit moth, and their parasitoid in southern norway. *Oikos*, 104:540–550, 2004.

V. Selås. Cyclic population fluctuations of herbivores as an effect of cyclic seed cropping of plants: the mast depression hypothesis. *Oikos*, 80:257–268, 1997.

L. Shalom, N. Samuels, S.and Zur, L. Shlizerman, H. Zemach, M. Weissberg, R. Ophir, E. Blumwald, and Sadka A. Alternate bearing in citrus: Changes in the expression of flowering control genes and in global gene expression in on- versus off-crop trees. *PLOS ONE*, 7(10):e46930, 2012.

D. Simokov and J. Pérez-Mercader. Noise induced oscillations and coherence resonance in a generic model of the nonisothermal chemical oscillator. *Sci. Rep.*, 3:2404, 2013.

A. R. E. Sinclair, J. M. Gosline, G. Holdsworth, C. J. Krebs, S. Boutin, J. N. M. Smith, R. Boonstra, and M. Dale. Can the solar cycle and climate synchronize the snowshoe hare cycle in canada? evidence from tree rings and ice cores. *Am. Nat.*, 141(2):173–198, 1993.

V. Small, R. J.and Marcström and T. Willebrand. Synchronous and nonsynchronous population fluctuations of some predators and their prey in central sweden. *Ecography*, 16:360–364, 1993.

R. V. Solé. *Phase Transitions*. Princeton Univ. Press,, Princeton, NJ, 2011.

L. Stone, R. Olinky, B. Blasius, A. Huppert, and B. Cazelles. Complex synchronization phenomena in ecological systems. *AIP Conf. Proc.*, 622(1):476–488, 2002.

T. Tchumatchenko and C. Clopath. Oscillations emerging from noise-driven steady state in networks with electrical synapses and subthreshold resonance. *Nat. Commun.*, 5:5512, 2014.

P. Turchin and S. P. Ellner. Living on the edge of chaos: population dynamics of fennoscandian voles. *Ecol.*, 81:3099–3116, 2000.

E. Wall, F. Guichard, and A.R. Humphries. Synchronization in ecological systems by weak dispersal coupling with time delay. *Theor. Ecol.*, 6:405–418, 2013.

J. Walter and G. Barkema. An introduction to monte carlo methods. *Physica A*, 418:78–87, 2015.

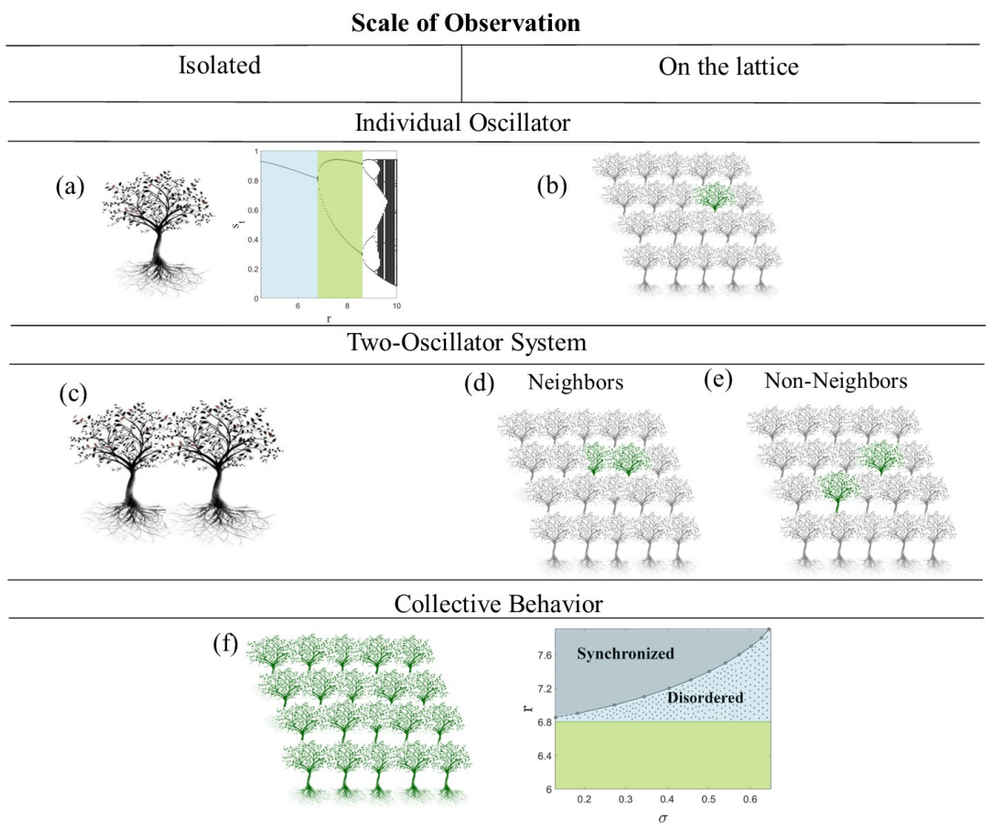

Figure 1: The scales of behavior studies in the paper. We analyse the time series of an individual oscillator (tree) in an isolated setting (the bifurcation diagram describes the deterministic dynamics of an isolated individual tree. The first bifurcation happens at $r = 6.8$) (a) and in the community (orchard) (b). Then we expand our view to include two-units, isolated (c) and in the orchard (d and e). Finally we study the collective dynamics of the entire orchard. The parameter phase diagram shows the collective dynamics of the system (f).

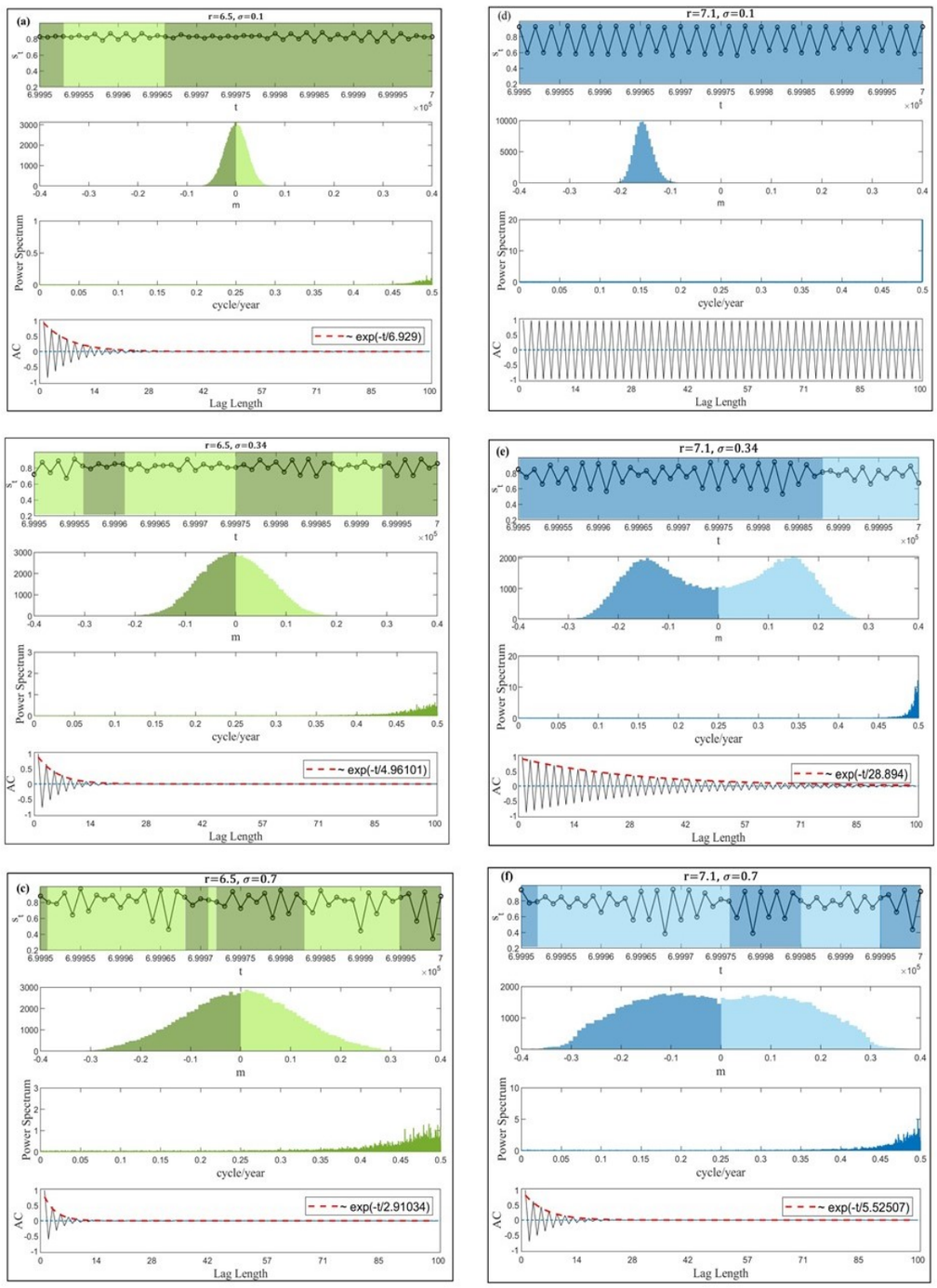

Figure 2: Dynamics of s_t for an isolated tree with $r = 6.5$ in the fixed point regime (left column) and $r = 7.1$ in the two-cycle regime under the effect of weak, medium, and strong noise (from top to bottom). Each box shows the time series, the distribution of the two cycle variable, the power spectrum, and the autocorrelation (AC) of the time series. The oscillator changes its phase under the effect of the noise (maximum happening in odd years versus even years). The change in phase is associated with the change in sign of the two-cycle variable. Different phases are color coded with different shades on the time series and the distributions of the two-cycle variable. In the fixed point regime, when the noise is too weak, the oscillator can stay close to its stable fixed point. Therefore the two cycle variable will be close to zero and it will be difficult to detect its phase. The time regions when this happens are left white in the time series graphs in figure 2. The time series in the left and right columns become increasingly similar as the noise intensity increases (first panels in all the boxes). The characteristic time for the decay of the amplitude of the autocorrelation (AC) decreases as the noise intensity increases. The characteristic times shown in this figure are measured from one simulation and are subject to statistical error (fourth panels in all the boxes).

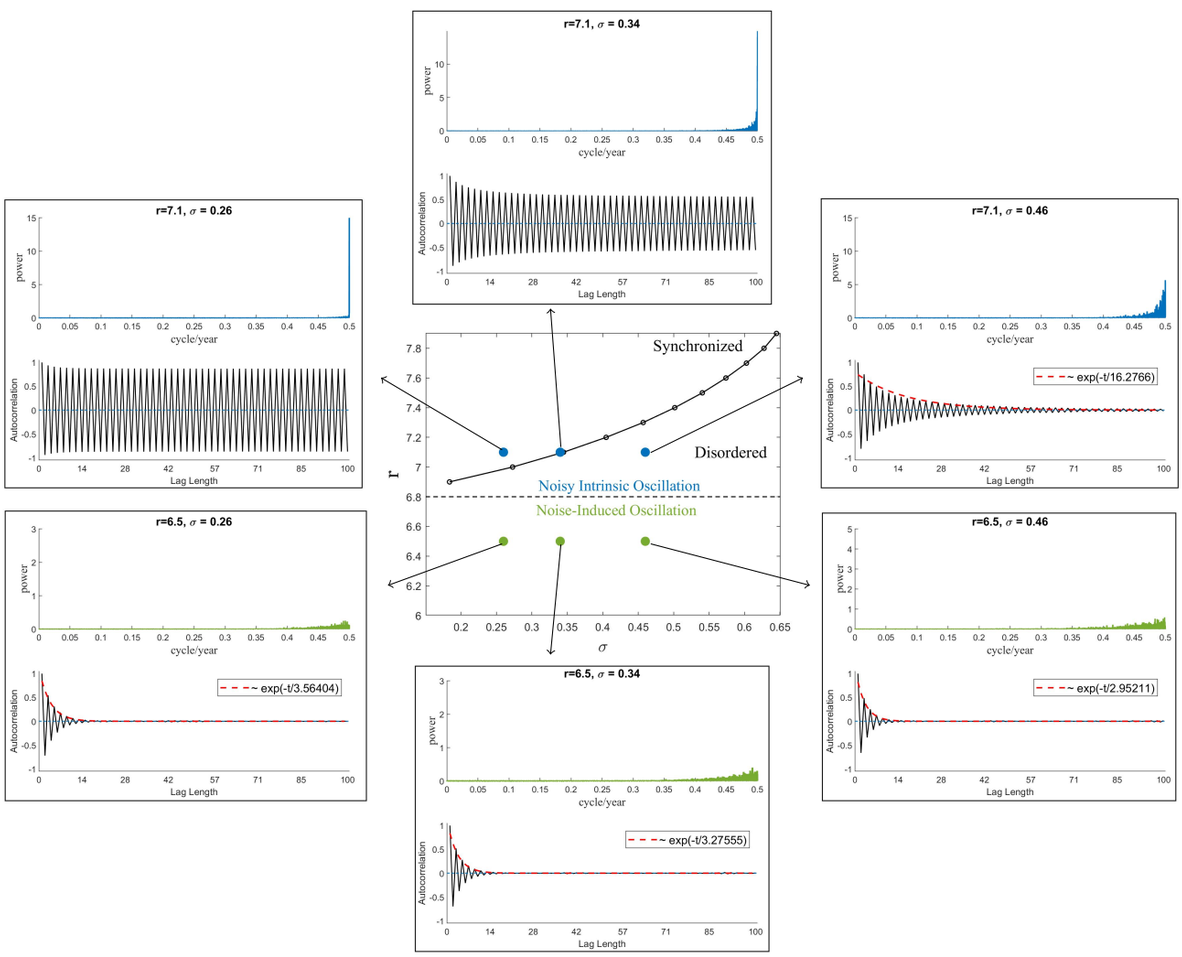

Figure 3: The power spectrum (note the different scales on the y-axis in each panel) and the autocorrelation for different noise values for $r = 6.5$ and $r = 7.1$ presented in the context of the phase transition. The plot at the center shows the $r - \sigma$ phase diagram. The black solid curve is the critical line separating the synchronized phase from the disordered phase.

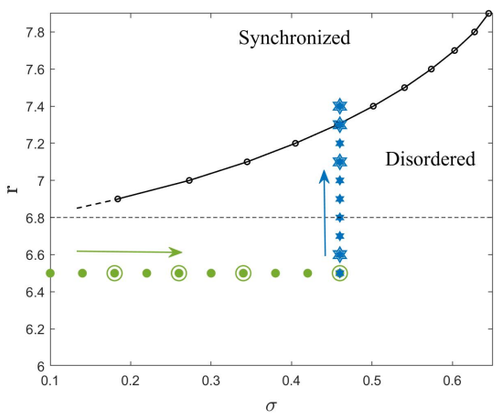

(a)

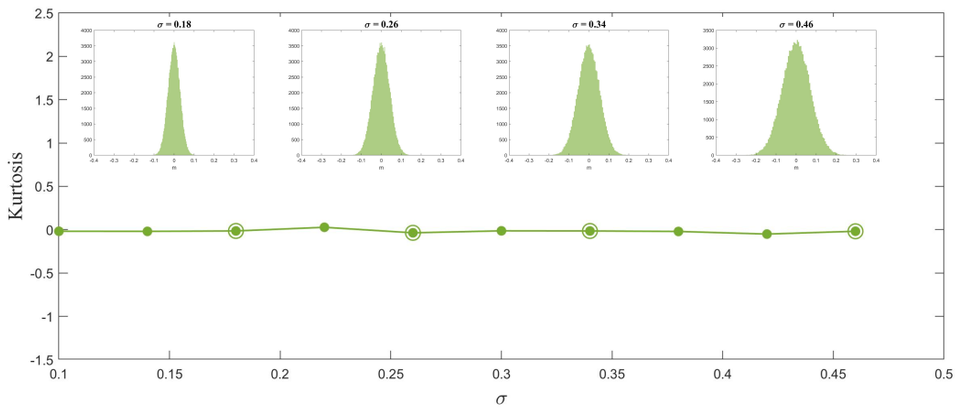

(b)

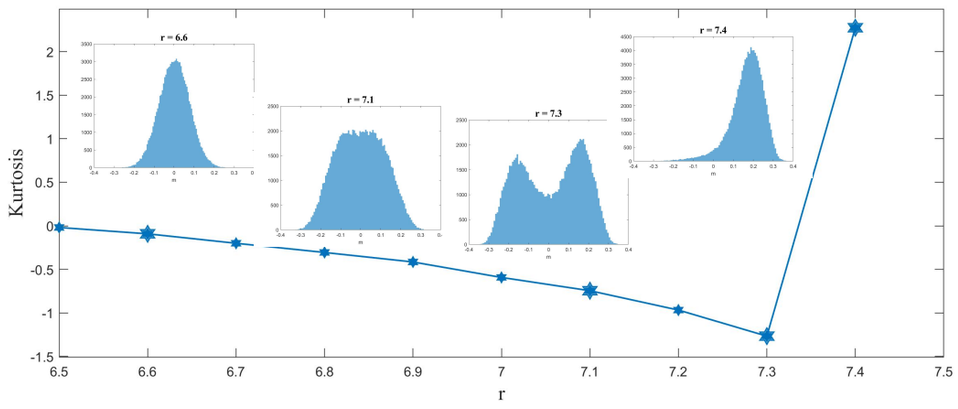

(c)

Figure 4: Panel (a) shows the parameters associated with panels (b) (green circles) and (c) (blue stars) in the context of the phase space. (b) The kurtosis of the distribution of the two-cycle variable is shown for different values of σ when $r = 6.5$. (c) The kurtosis for different values of r when $\sigma = 0.46$. The insets in both (b) and (c) show four samples of the distribution of the two-cycle variable for values of σ and r indicated with larger symbols on all the panels.

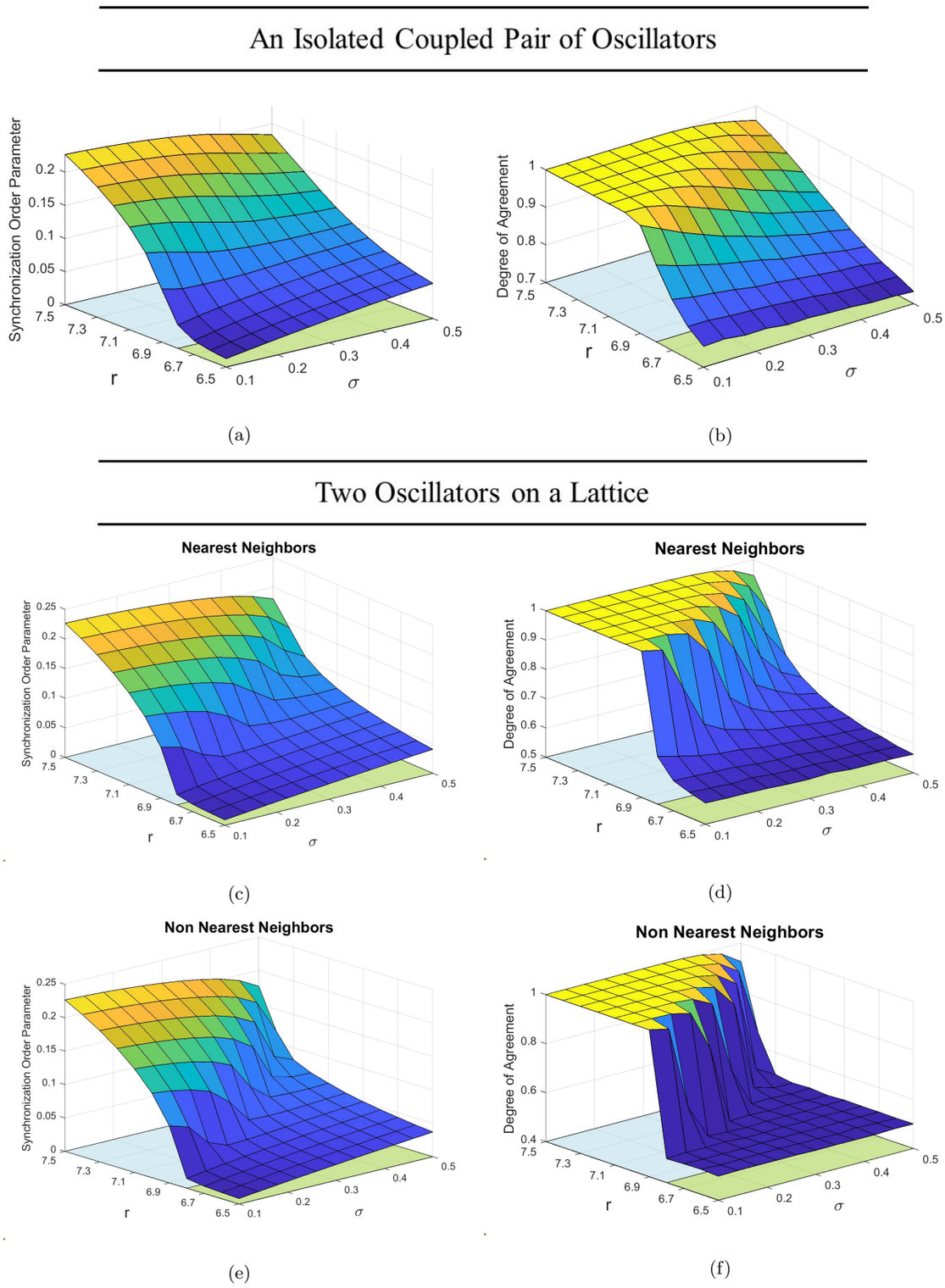

Figure 5: Measures of synchrony for two trees: (a) the synchronization Order Parameter as a function of r (the model's rate) and σ (noise intensity) for a pair of isolated coupled trees, (b) the Degree of Agreement as a function of r and σ fora pair of isolated coupled trees. (c) and (e) the synchronization Order Parameter as a function of r and σ for two nearest neighboring and non nearest neighboring trees inside an orchard respectively. (d) and (f) The Degree of Agreement as a function of r and σ for two nearest neighboring and non nearest neighboring trees inside an orchard respectively. The green shaded area in the $r-\sigma$ plane shows the fixed point regime while the blue shaded area shows the two-cycle regime. $\kappa = 0.15$ and $l = 7$ for all six panels.

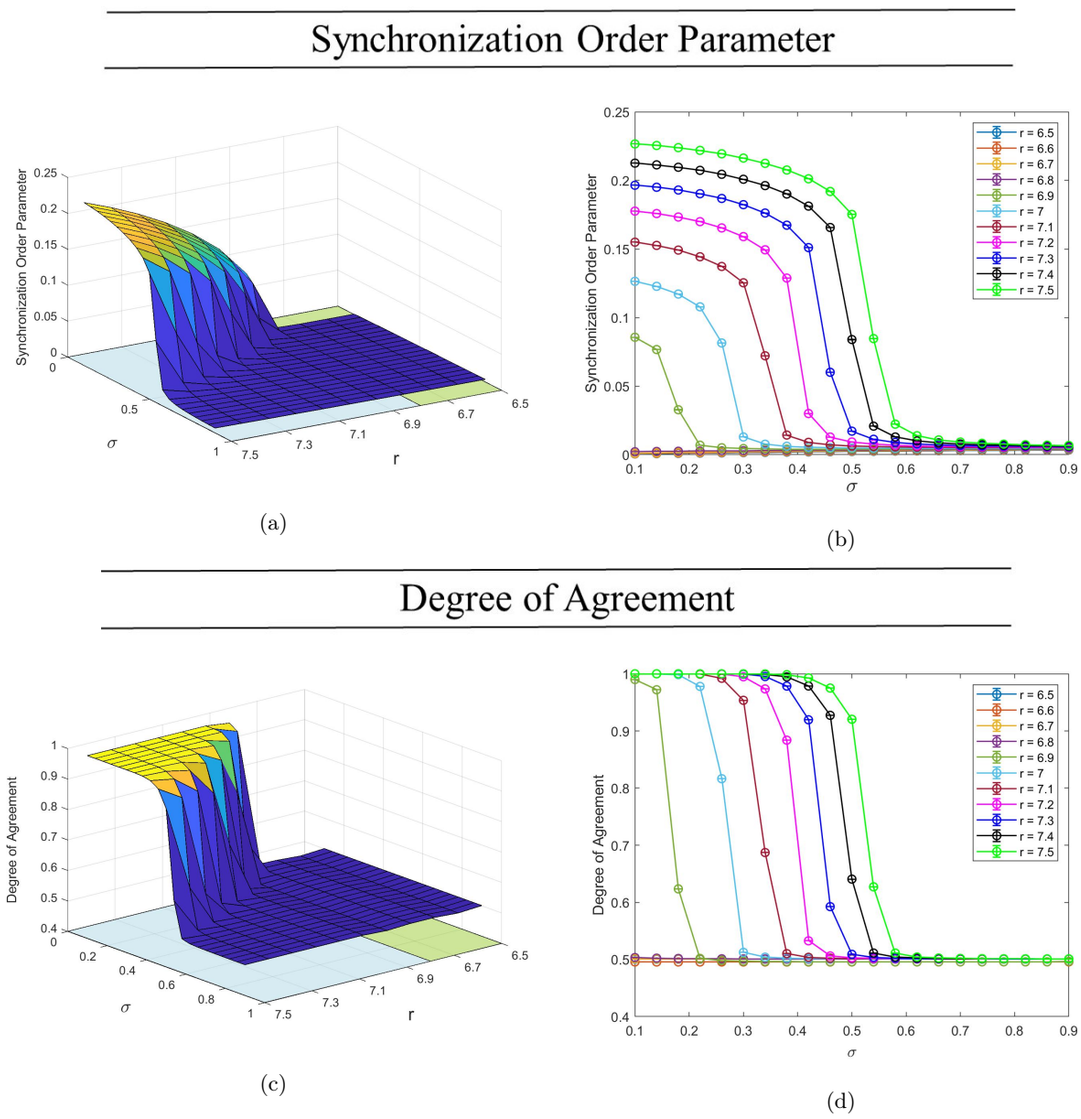

Figure 6: Measure of synchrony for the entire lattice: (a) and (b) the synchronization Order Parameter of the entire orchard as a function of r (the model's rate) and σ (noise intensity) (a) and as a function of σ for different r values (b). (c) and (d) the Degree of Agreement for the entire orchard as a function of r (the model's rate) and σ (noise intensity) (c) and and as a function of σ for different r values (d). The green shaded area in the $r-\sigma$ plane shows the fixed point regime while the blue shaded area shows the two-cycle regime. $\kappa = 0.15$ and $l = 7$ for all panels.